Available online at www.sciencedirect.com

ScienceDirect

IFAC Papers Online CONFERENCE PAPER ARCHIVE

IFAC PapersOnLine 51-24 (2018) 818–823

Fault detection and isolation for Unmanned Aerial Vehicle sensors by using extended PMI filter

Dingfei Guo * **Yulin Wang** ** **Maiying Zhong** *** **Yan Zhao** *

* *School of Instrumentation Science and Opto-electronic Engineering, Beihang University, Beijing 100191, P. R. China.*
** *School of Automation Science and Engineering, Beihang University, Beijing 100191, P. R. China.*
*** *College of Electrical Engineering and Automation, Shandong University of Science and Technology, Qingdao 266590, P. R. China.*

Abstract: Fault detection and isolation (FDI) plays an important role in guaranteeing system safety and reliability for unmanned aerial vehicles (UAVs). This paper focuses on developing a method for detecting UAV sensor faults by using existing sensors, such as pitot tube, gyro, accelerometer and wind angle sensor. We formulate the kinematics as a nonlinear state space system, which requires no dynamic information and thus is applicable to all aircraft. To illustrate the method, we investigate five fault-detection scenarios, namely, faulty pitot tube, angle-of-attack sensor, sideslip sensor, accelerometer and gyro, and design a FDI structure including five faulty sensors. Then, considering the unknown disturbance, the proportional and multiple integral (PMI) fault detection filter (FDF) is proposed for the state and input estimation. A structure including two residuals are employed to detect and isolate the faults of the proposed faulty sensors. Finally, the performance of the proposed methodology is evaluated through flight experiments of the UAV.

Keywords: Unmanned aerial vehicles, kinematics model, proportional multiple integral, sensors fault detection and isolation.

1. INTRODUCTION

The mobility and economic efficiency of unmanned aerial vehicles (UAV) afford them a high number of applications Rossi (2016). UAV is a typical multi-sensor system, including inertial measurement unit (IMU), Global Positioning System (GPS), Air Data System (ADS), magnetometer, etc. Sensor faults have catastrophic consequences for the systems that operate under feedback control. In order to achieve precise control and navigation of the UAV, the reliability of the sensor system must be ensured. For the UAV application, it is highly desirable to develop an aircraft flight control system with reconfigurable capabilities: able to detect and isolate failures of sensors and then to apply a control algorithm that has been specially designed for the current failure mode status. Traditional approaches to sensor fault tolerance for UAV have been based on hardware redundancy Hajiyev and Caliskan (2003). Multiple hardware components provide protection against damages. Such schemes operate in a triplicated or quadruplicated redundancy configuration. However, faults on any individual pitot tube are also likely to occur on other pitot tubes under certain weather conditions.

For this purpose, various approaches have been proposed in the literatures Brumback adn Srinath (1987). A general approach for UAV sensor fault detection is hypothesis testing of the innovation Hajiyev and Caliskan (2003), Cao et al. (2017). Already back to the 1970s, the use of analytical redundancy was employed for sensor fault identification as reported for example in Deckert et al. (1977). There, a bank of sequential probability ratio tests compute probabilities on whether a sensor is faulty over a time-window of residuals. However, these approaches cannot isolate the sensor fault from actuator faults. Another technique is the multiple model adaptive estimation technique Maybeck (1999) based on an idea from Magill (1965). Fault estimation Chen et al. (2016) was used for UAV sensor FDI and is easily influenced by the disturbance. The genetic algorithm back propagation based neural-network Chen et al. (2017) and other data driven methods Fan et al. (2017) have large computation burdens in online operation. Castaldi et al. (2016) proposed a nonlinear geometric approach for the UAV actuators and sensors based on the mathematical model. However, this method need the identification parameters of the model.

One approach to detecting sensor faults is to use measurements from a set of sensors to estimate a state or input and then compare the estimate with the measurement from a suspect sensor that is not used for the estimation. In the case where the suspect sensor corresponds to a state of a dynamic system, state estimation techniques, such as the

⋆ This work was supported in part by the National Natural Science Foundation of China under Grants (61333005, 61733009,61673032), and the Research Fund for the Taishan Scholar Project of Shandong Province of China. Corresponding author: Maiying Zhong(myzhong@buaa.edu.cn).

10.1016/j.ifacol.2018.09.669

Kalman filter and its nonlinear variants, can be used. In the case where the suspect sensor corresponds to an input of a dynamic system, state estimation techniques that include input estimation can be used. The present paper focuses on above sensor FDI method for UAV. In this application, two distinct classes of sensors are available. Inertial sensors including rate gyros and accelerometers measure the motion of the vehicle relative to an inertial frame. Noninertial sensors include position measurements from GPS as well as aerodynamic sensors, such as a pitot tube for measuring forward velocity relative to the air and angle-of-attack (α) and sideslip (β) sensors for measuring the direction of the relative wind in the body frame. In this paper we use combinations of inertial and aerodynamic sensors along with fault detection filter (FDF) techniques to detect and isolate sensor faults. For the unknown input estimation in the second scenario, a proportional multiple integral(PMI) based FDF described is used Gao and Ding (2007).

The remainder of this paper is structured as follows. Following a brief problem statement in Section II, the method for extended PMI based FDI is proposed in Section III. Finally, the presented approach is validated using actual flight data from the Ultra Stick UAV.

2. PROBLEM FORMULATION

Before developing the aircraft equations of motion, it is necessary to define reference frames and sign conventions. All reference frames are right handed and with mutually orthogonal axes. Inertial frame (i frame) has its origin at the center of the earth and not rotating with the fixed stars. The local level NED (North-East-Down) frame is selected as navigation frame (n-frame). Body frame (b frame) $x_b y_b z_b$. Origin is at the aircraft center of gravity, with positive x_b axis pointing forward through the nose of the aircraft, positive y_b axis out the right wing, and positive z_b axis through the underside. Wind axes $X_w Y_w Z_w$. Origin is at the aircraft center of gravity, with positive X_w axis forward and aligned with the air-relative velocity vector, positive Y_w axis out the right side of the aircraft, and positive Z_w axis through the underside in the $X_w Y_w$ plane in body axes.

The flat-earth, body-axes 6-Dof equations of the UAV can be expressed in body frame as follows Stevens et al. (2016)

$$\begin{cases} \dot{u} = rv - qw - g\sin\theta + (F_{Ax} + F_T)/m \\ \dot{v} = pw - ru + g\sin\phi\cos\theta + (F_{Ay})/m \\ \dot{w} = qu - pv + g\cos\phi\cos\theta + (F_{Az})/m \\ \dot{p} = [L + (I_{yy} - I_{zz})qr + I_{xz}(\dot{r}p + pq)]/I_{xx} \\ \dot{q} = [M + (I_{zz} - I_{xx})rp + I_{xz}(r^2 + p^2)]/I_{yy} \\ \dot{r} = [R + (I_{xx} - I_{yy})pq + I_{xz}(\dot{p}p + qr)]/I_{zz} \end{cases} \tag{1}$$

where $\mathbf{V}_a = [\, u \;\; v \;\; w \,]^T$ denotes the body-axis airspeed component, $\Omega = [\, p \;\; q \;\; r \,]^T$ stands for the angular velocity vector of the body-axis component, Euler attitude angles $\Phi = [\, \phi \;\; \theta \;\; \psi \,]^T$ stands for roll, pich and yaw respectively. $\mathbf{F}_A = [\, F_{Ax} \;\; F_{Ay} \;\; F_{Az} \,]^T$ stands for the aerodynamic force and $\mathbf{F}_A = \mathbf{f}_A(\mathbf{V}_a, \delta_e, \delta_a, \delta_r)$, $\delta_e, \delta_a, \delta_r$ denotes the control surface position of the elevator, aileron and rudder, respectively. F_T is the propulsive force. $\mathbf{M} = [\, L \;\; M \;\; R \,]^T$ stants for the aerodynamic moment and $\mathbf{M} = \mathbf{f}_M(\mathbf{V}_a, \delta_e, \delta_a, \delta_r)$. $I_{xx}, I_{yy}, I_{zz}, I_{xz}$ are the moments of inertia.

And the kinematic equations is given below

$$\begin{cases} \dot{\phi} = p + \tan\theta(q\sin\phi + r\cos\phi) \\ \dot{\theta} = q\cos\phi - r\sin\phi \\ \dot{\psi} = (q\sin\phi + r\cos\phi)/\cos\theta \\ \alpha = \tan^{-1}\left(\dfrac{w}{u}\right) \\ \beta = \sin^{-1}\left(\dfrac{v}{\sqrt{u^2 + v^2 + w^2}}\right) \end{cases} \tag{2}$$

(1) and (2) give the dynamic and kinematic equation of the UAV. Aerodynamic forces and moments acting on the aircraft result from the relative motion of the air and the aircraft. Generally, modern computational methods and wind-tunnel testing can provide, in many instances, comprehensive data about the aerodynamic characteristics of an aircraft. Therefore, a nonlinear model in terms of the state variables including $\mathbf{V}_a, \Omega, \Phi$ and the input $\delta_e, \delta_a, \delta_r$ will be constructed. In this paper, for the FDI of the UAV, IMU is used to measure accelerations and angular rates.

$$\begin{aligned} \mathbf{a}_m &= \frac{1}{m}[\, F_{Ax} + F_T \;\; F_{Ay} \;\; F_{Az} \,]^T \\ \omega_m &= [\, p \;\; q \;\; r \,]^T \end{aligned} \tag{3}$$

$\mathbf{a}_m$ and ω_m are outputs of accelerometers and rate gyroscopes. In this model, the input is replaced by the measurements of the accelerometer and the gyro. It should be pointed out that there are multiple possible sources of error in the accelerometer and rate gyroscope measurements, such as calibration errors, alignment errors, and sensor noise, which can be modeled as

$$\begin{aligned} \mathbf{a}_m &= \mathbf{a} + \mathbf{W}^{\mathbf{a}} \\ \omega_m &= \omega + \mathbf{W}^{\omega} \end{aligned}$$

where

$$\mathbf{a} = [\, a_x \;\; a_y \;\; a_z \,]^T \qquad \omega = [\, \omega_x \;\; \omega_y \;\; \omega_z \,]^T$$

denote specific outputs. $\mathbf{W}^{\mathbf{a}}$ and $\mathbf{W}^{\omega}$ are zero mean Gauss white noise. Therefore (1) is transformed to airspeed kinematics equation.

$$\begin{aligned} \begin{bmatrix} \dot{u} \\ \dot{v} \\ \dot{w} \end{bmatrix} &= \begin{bmatrix} 0 & \omega_y & -\omega_z \\ \omega_x & 0 & -\omega_y \\ \omega_z & -\omega_x & 0 \end{bmatrix} \begin{bmatrix} u \\ v \\ w \end{bmatrix} + C_n^b \begin{bmatrix} 0 \\ 0 \\ g \end{bmatrix} + \begin{bmatrix} a_x \\ a_x \\ a_x \end{bmatrix} \\ \begin{bmatrix} p \\ q \\ r \end{bmatrix} &= \begin{bmatrix} \omega_x \\ \omega_y \\ \omega_z \end{bmatrix} \end{aligned} \tag{4}$$

where C_n^b is the transfer matrix from the navigation frame to the body frame. Generally in aircraft control systems, the aerodynamic parameters can provide more accurate results than the measurements of the IMU. However, for the FDI of UAVs, which is different from aircraft control, the airborne IMU can satisfy the required precision and help to reduce the complexity of the FDI system. And more importantly, based on the replaced equation (4) and the kinematic equation (2), we can easily design the FDI system for the UAV's sensors, including the IMU, the pitot tube, the α-sensor and β-sensor. Fig.1 shows the structure of the proposed FDI system.

In Fig.1, this paper designs five different models and filters for each faulty sensor. Each model can generate an

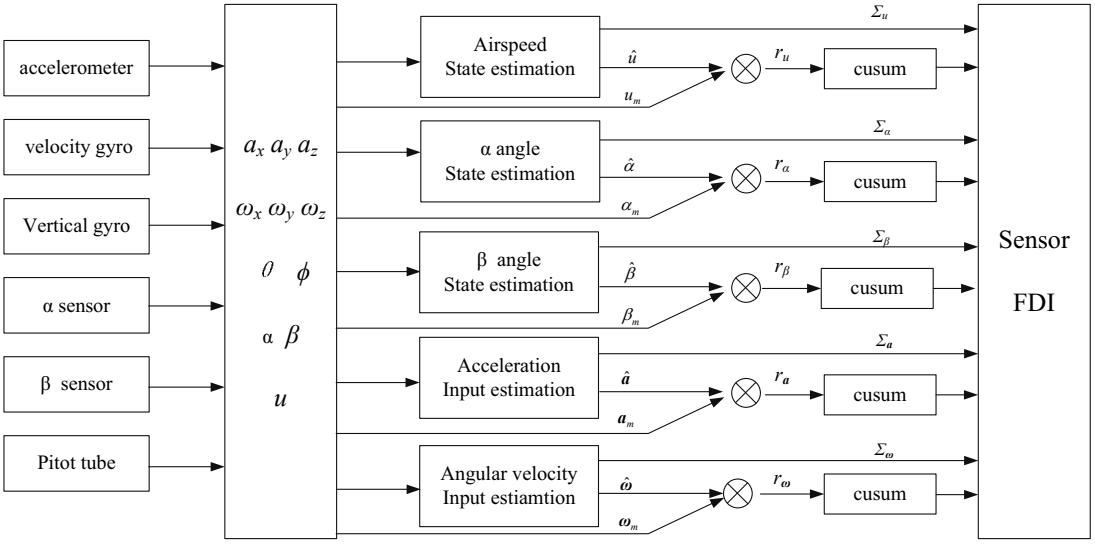

Fig. 1. Structure of FDI system for UAV sensors

innovation based residual and an estimation result of the corresponding sensor. Another residual is the difference between the estimation result and the actual output of the sensor. For example, for the faulty pitot tube, this paper constructed the state equation based (4) and output equation using the measurements of the α-sensor and β-sensor. Then two different residuals can be acquired using the state estimation, such as the Kalman, and then the FDI of the pitot tube can be achieved. Based on the formulation, A continuous-time state-space model can be formulated as

$$\begin{aligned}\dot{\mathbf{x}}(t) &= \mathbf{f}_c(\mathbf{x}(t), \mathbf{u}_k(t), \mathbf{u}_u(t)) + D_1(t)\mathbf{w}(t)\\ \mathbf{y}(t) &= \mathbf{h}(\mathbf{x}(t)) + D_2(t)\mathbf{v}(t)\end{aligned} \tag{5}$$

where $\mathbf{x}$ is the state, $\mathbf{u}_k$ is the known input, $\mathbf{u}_u$ is the unknown input, $\mathbf{w}$ is the process noise, $\mathbf{y}$ is the output measurement, and $\mathbf{v}$ is the measurement noise, and the functions $\mathbf{f}_c$ and $\mathbf{h}$ are known. It should be noted that $\mathbf{u}_k$ and $\mathbf{u}_u$ are not the traditional control inputs. We used the measurements of IMU to replace the control inputs (3). And there are some faults occurred in IMU possibly. Therefore, when the inertial sensors are the estimated objects, they are defined as the unknown inputs $\mathbf{u}_u$. Otherwise defined as the known inputs $\mathbf{u}_k$. Table 1 defines $\mathbf{x}$, $\mathbf{u}_k$, $\mathbf{u}_u$ and $\mathbf{y}$ for five fault-detection scenarios, in particular, faulty pitot tube, α-sensor, β-sensor, accelerometer and rate gyro. It should pointed out that the five different sensors are located in the states or the inputs. Therefore, in order to obtain the estimation of the faulty sensors, we should design FDF methods for the FDI system.

3. EXTENDED PMI BASED FDI FOR UAV

In Section II, the FDI system for UAV sensors is formulated as a problem of state and input estimation. We use the extended Kalman filter (EKF) for state estimation and PMI based state estimation for input estimation. The well known EKF is familiar with us and it is the spacial case of the PMI based estimation. Therefore, we directly give the PMI based FDF.

Table 1. Scenarios for sensor fault detection

Faulty Sensor	$\mathbf{x}$	$\mathbf{y}$	$\mathbf{u}_k$	$\mathbf{u}_u$
Pitot tube	u, v, w	α, β	a_x, a_y, a_z $\omega_x, \omega_y, \omega_z$ ϕ, θ	
α-sensor	u, v, w	u, β	a_x, a_y, a_z $\omega_x, \omega_y, \omega_z$ ϕ, θ	
β-sensor	u, v, w	u, α	a_x, a_y, a_z $\omega_x, \omega_y, \omega_z$ ϕ, θ	
Accelerometer	u, v, w	u, α, β	$\omega_x, \omega_y, \omega_z$ ϕ, θ	a_x, a_y, a_z
Rate Gyro	u, v, w	u, α, β	a_x, a_y, a_z ϕ, θ	$\omega_x, \omega_y, \omega_z$

3.1 Design of Extended PMI FDF

In the case where the input is partially or fully unknown, (5) does not explicitly account for the unknown input $\mathbf{u}_u$. The effect of $\mathbf{u}_u(t)$ can be included in the process noise $\mathbf{w}(t)$ by a suitable choice of the covariance matrix of the system noise. A more effective approach is to estimate $\mathbf{u}_u(t)$ and include it in (5) with its estimate $\hat{\mathbf{u}}_u(t)$. In this case, the unknown input $\mathbf{u}_u(t)$ is approximated by the following polynomial function

$$\mathbf{u}_u(t) = B_0 + B_1 t + B_2 t^2 + \cdots + B_{q-1} t^{q-1} \tag{6}$$

where $B_i (i = 0, 1, \cdots, q-1)$ are unknown constant vectors with $q \geq 1$. Define

$$\xi_i(t) = \mathbf{u}_u^{(q-i)}(t)\ \ (i = 1, 2, \cdots q) \tag{7}$$

It follows from (6) and (7) that

$$\begin{cases} \dot{\xi}_1(t) = 0 \\ \dot{\xi}_2(t) = \xi_1(t) \\ \vdots \\ \dot{\xi}_q(t) = \xi_{q-1}(t) \end{cases} \tag{8}$$

Augmenting (5) and (8) yields

$$\dot{\bar{\mathbf{x}}}(t) = \bar{\mathbf{f}}_c(\bar{\mathbf{x}}(t), \mathbf{u}_k(t)) + D_1(t)\mathbf{w}(t)$$

$$\mathbf{y}(t) = \bar{\mathbf{h}}(\bar{\mathbf{x}}(t)) + D_2(t)\mathbf{v}(t) \tag{9}$$

where

$$\bar{\mathbf{x}}(t) = [\, \mathbf{x}^T(t)\ \xi_1^T(t)\ \xi_2^T(t)\ \cdots\ \xi_q^T(t)\,]^T$$

$$\bar{\mathbf{f}}_c(\bar{\mathbf{x}}, \mathbf{u}_k) = \begin{bmatrix} \mathbf{f}_c(\mathbf{x}, \mathbf{u}_k, \xi_q) \\ 0\ 0\ \cdots\ 0\ 0 \\ 0\ 1\ \cdots\ 0\ 0 \\ \vdots\ \vdots\ \ddots\ \vdots\ \vdots \\ 0\ 0\ \cdots\ 1\ 0 \end{bmatrix}$$

$$\bar{\mathbf{h}}(\bar{\mathbf{x}}) = \mathbf{h}(\mathbf{x})$$

In order to implement these equations in a discrete-time filter, a first-order discretization is used

$$\begin{aligned} \bar{\mathbf{x}}(k+1) &= \bar{\mathbf{f}}(\bar{\mathbf{x}}(k), \mathbf{u}_k(k)) + \bar{D}_1\mathbf{w}(k) \\ \mathbf{y}(k) &= \bar{\mathbf{h}}(\mathbf{x}(k)) + D_2\mathbf{v}(k) \end{aligned} \tag{10}$$

where k is the time step, $\bar{D}_1 = T_s D_1$, T_s is the sampling time.

$$\bar{\mathbf{f}}(\bar{\mathbf{x}}, \mathbf{u}_k) = \begin{bmatrix} \mathbf{f}(\mathbf{x}, \mathbf{u}_k, \xi_q) \\ 0\ 1\ \cdots\ 0\ 0 \\ 0\ T\ \cdots\ 0\ 0 \\ \vdots\ \vdots\ \ddots\ \vdots\ \vdots \\ 0\ 0\ \cdots\ T\ 1 \end{bmatrix}$$

For $k = 1, 2, ...$, perform the following steps:

1. Perform the time update of the state estimate and estimation-error covariance as follows:

$$\begin{aligned} \check{\bar{\mathbf{x}}}(k) &= \bar{\mathbf{f}}(\hat{\bar{\mathbf{x}}}(k-1), \mathbf{u}_k(k-1)) \\ \check{\bar{P}}(k) &= \bar{F}(k-1)\hat{\bar{P}}(k-1)\bar{F}^T(k-1) + \hat{\bar{D}}_1\hat{\bar{D}}_1^T \end{aligned}$$

where

$$\bar{F}(k-1) = \frac{\partial \bar{\mathbf{f}}}{\partial \bar{\mathbf{x}}}|_{\hat{\bar{\mathbf{x}}}(k-1), \mathbf{u}_k(k-1)}$$

2. At time k, incorporate the measurement $\mathbf{y}(k)$ into the state estimate and estimation covariance as follows:

$$\begin{aligned} \bar{K}(k) &= \check{\bar{P}}(k)\bar{H}(k)^T(\bar{H}(k)\check{\bar{P}}(k)\bar{H}(k)^T + D_2D_2^T)^{-1} \\ \hat{\bar{\mathbf{x}}}(k) &= \check{\bar{\mathbf{x}}}(k) + \bar{K}(k)(\mathbf{y}(k) - \bar{\mathbf{h}}(\check{\bar{\mathbf{x}}}(k))) \\ \hat{\bar{P}}(k) &= \check{\bar{P}}(k) - \check{\bar{P}}(k)\bar{H}(k)^T \\ &\quad \times(\bar{H}(k)\check{\bar{P}}(k)\bar{H}(k)^T + D_2D_2^T)\bar{H}(k)\check{\bar{P}}(k) \end{aligned}$$

where

$$\bar{H}(k) = \frac{\partial \bar{\mathbf{h}}}{\partial \bar{\mathbf{x}}}|_{\hat{\bar{\mathbf{x}}}(k)}$$

Table 2 lists the on-board sensors for fault detection. The matrices D_1 and D_2 are determined using Table 2 and are given as follows.

Scenario 1) Faulty pitot tube:

$$D_1 = [\, D_\omega\ D_{\mathbf{a}}\,], D_2 = diag(\sigma_\alpha, \sigma_\beta) \tag{11}$$

where

Table 2. The additive noise for each sensor is assumed to be white Gaussian

Sensors	Measurements	Variance of Noise
Pitot tube	u	σ_u^2
Rate Gyro	$\omega_x, \omega_y, \omega_z$	σ_ω^2
Accelerometers	a_x, a_y, a_z	σ_a^2
α-sensor	α	σ_α^2
β-sensor	β	σ_β^2

$$\begin{aligned} D_\omega &= \begin{bmatrix} 0 & -w & v \\ w & 0 & -u \\ -v & u & 0 \end{bmatrix} diag(\sigma_\omega, \sigma_\omega, \sigma_\omega) \\ D_{\mathbf{a}} &= diag(\sigma_a, \sigma_a, \sigma_a) \end{aligned} \tag{12}$$

Scenario 2) Faulty α-sensor: D_1 is given by (12) and

$$D_2 = diag(\sigma_u, \sigma_\beta) \tag{13}$$

Scenario 3) Faulty β-sensor: D_1 is given by (12) and

$$D_2 = diag(\sigma_u, \sigma_\alpha) \tag{14}$$

Scenario 4) Faulty accelerometer:

$$D_1 = D_\omega, D_2 = diag(\sigma_u, \sigma_\alpha, \sigma_\beta) \tag{15}$$

Scenario 5) Faulty rate gyro:

$$D_1 = D_{\mathbf{a}}, D_2 = diag(\sigma_u, \sigma_\alpha, \sigma_\beta) \tag{16}$$

Rewrite the gain $\bar{K}$ as

$$\bar{K}(k) = [\, \bar{K}_P(k)^T\ \bar{K}_1(k)^T\ \cdots\ \bar{K}_q(k)^T\,]^T$$

where $\bar{K}_P(k)$ denotes the proportional gain, $\bar{K}_i(k)$ $(i = 1, 2, \cdots, q)$ denote integral gains. Then $\hat{\bar{\mathbf{x}}}(k)$ can be re-expressed in the following form

$$\begin{cases} \hat{\mathbf{x}}(k) = \mathbf{f}_c(\check{\mathbf{x}}(k), \mathbf{u}_k(k), \hat{\xi}_q(k)) + \bar{K}_P(k)(\mathbf{y}(k) - \mathbf{h}(\check{\mathbf{x}}(k)) \\ \hat{\xi}_1(k) = \bar{K}_1(k)(\mathbf{y}(k) - \mathbf{h}(\check{\mathbf{x}}(k)) + \hat{\xi}_1(k-1) \\ \hat{\xi}_2(k) = \bar{K}_2(k)(\mathbf{y}(k) - \mathbf{h}(\check{\mathbf{x}}(k)) + T\hat{\xi}_1(k) + \hat{\xi}_2(k-1) \\ \qquad\qquad \vdots \\ \hat{\xi}_q(k) = \bar{K}_q(k)(\mathbf{y}(k) - \mathbf{h}(\check{\mathbf{x}}(k)) + T\hat{\xi}_{q-1}(k) + \hat{\xi}_q(k-1) \end{cases}$$

that is the so-called extended PMI based FDF.

It is seen that there are multi-integral information included in $\hat{\xi}_i(k)(i = 1, 2..., q)$. That is to say, $\hat{\xi}_i(k)$ is an estimation of the $(q-i)$th derivation of the unknown input $\mathbf{u}_u(k)$ in the form (6), and $\hat{\xi}_q(k)$ is an estimation of $\mathbf{u}_u(k)$. At the same time, the estimation of $\mathbf{x}(k)$ includes innovation $\mathbf{y}(k) - \mathbf{h}(\check{\mathbf{x}}(k)$ and input estimation $\hat{\xi}_q(k)$. Therefore, choosing suitable $q \geq 1$, the proposed method can achieve accurate state estimation $\hat{\mathbf{x}}(k)$ with the unknown input $\hat{\mathbf{u}}_u(k)$.

It should be noted that when the faulty sensor is defined as state and the input is known, the unknown input $\hat{\mathbf{u}}_u(k)$ is not exist. For the PMI based FDF

$$\hat{\mathbf{u}}_u(k) = \mathbf{0} \tag{17}$$

Therefore, the extended PMI based FDF can be regressed to the well known EKF. In other words, the EKF is the special case of the PMI based FDF when the unknown input is absent.

3.2 Multisensor Fault Detection and Isolation

This paper uses the difference between the virtual "measurements", estimated using other sensors, and the outputs provided by real sensors to indicate the fault information of the sensors.

For the extended PMI based FDF of the accelerometers, the velocity gyros, the pitot tube and the wind vanes, define the residual as

$$\Sigma_i(k) = \mathbf{y}_i(k) - \hat{\mathbf{y}}_i(k) = \mathbf{y}_i(k) - \mathbf{h}(\hat{\mathbf{x}}_i(k)) \tag{18}$$

where i stands for the different sensors $u, \alpha, \beta, \mathbf{a}, \omega$. Note that the output $\Sigma_i(k)$ did not include the information of the faulty sensor. If the other used sensors are healthy, the following result is easily achieved.

$$\Sigma_i(k) \sim N(0, R_{\Sigma_i}) \tag{19}$$

Introduce the residual evaluation

$$J_{\Sigma_i}(k) = \frac{1}{N+1} \sum_{j=k-N}^{k} \Sigma_i^T(j) R_{\Sigma_i}^{-1}(j) \Sigma_i(j) \tag{20}$$

Based on (19), the $J_{\Sigma_i}(k)$ follows a central χ^2 distribution with corresponding degrees of freedom. For example, the degree of the airspeed estimation is 2. Therefore, we can use $J_{\Sigma_i}(k)$ as an evaluation function and monitor the status of the sensors. Choose a false alarm rate (FAR) ε_i; then, the threshold can be determined based on the χ^2 distribution.

$$J1_{\Sigma_i} = \chi^2_{\varepsilon_i} \tag{21}$$

On the other hand, define the residual r_i as

$$r_i(k) = i_m(k) - \hat{i}(k) \tag{22}$$

where i stands for the different sensors $u, \alpha, \beta, \mathbf{a}, \omega$, $i_m(k)$ is the measurement of the sensor, $\hat{i}(k)$ is the estimation of the sensor output. It should be noted that, $\hat{\alpha}$ and $\hat{\beta}$ are not estimated directly. They are calculated by $\hat{u}, \hat{v}, \hat{w}$ using (2).

The fault detection procedure is designed to determine whether the observed changes in the residual signal $r_i(k)$ can be justified in terms of the disturbance (measurement noise) or modeling uncertainty. We use the well-known filter used for the detecting the abrupt change of $r_i(k)$, named Cumulative Sum (CUSUM) filter Basseville and Nikiforov (1993). The CUSUM filter is defined by the following equation Campa et al. (2002):

$$J_{r_i}(k) = sup\left(0, J_{r_i}(k-1) - \frac{\tau(\tau - 2r_i(k))}{2\sigma_0^2}\right) \tag{23}$$

where The values of the parameter τ is the value of the expected fault amplitude. σ_0 is the standard deviation which is calculated in advance. The fault detection threshold for the CUSUM signal $J_{r_i}(k)$ was selected as a compromise between the need for a fast fault detection and the need for low false alarm rates. An acceptable trade-off was found by setting the threshold equal to 1.5 times the maximum value of the CUSUM signal observed in fault-free conditions for a validation simulated flight.

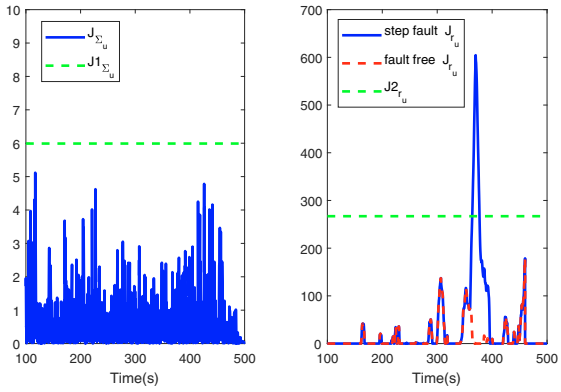

Fig. 2. The pitot tube fault diagnosis

$$J2_{r_i} = 1.5 \cdot \max\left(J_{r_i}(k)\right) \tag{24}$$

Based on (18) and (22), the fault detection logic of the UAV sensors can be expressed as Table 3. Where $\times$ means if the evaluation functions go beyond the thresholds, this detect logic will alarm, i.e. $J_{\Sigma_i}(k) > J1_{\Sigma_i}$ or $J_{r_i}(k) > J2_{r_i}$. $\surd$ stands for no alarm happened. For example, if the pitot tube is faulty, the evaluation function J_{r_u} will exceed the threshold $J2_{r_u}$ and J_{Σ_u} keeps below the threshold $J1_{\Sigma_u}$. According to indication of these evaluation functions, we can easily detect these sensors' faults and isolate them.

4. SIMULATION

The research platform used in this study is the Ultra Stick 25e UAV. The onboard avionics system, features a an Analog Devices iSensor ADIS16405 IMU, accelerometers with 50mg initial bias error and 9 mg RMS noise, and gyroscopes with 3°/sec initial bias error and 0.9°/sec RMS output noise.

4.1 Fault detection for pitot tube failure

In the following cases, the pitot tube fails by becoming stuck at the constant value $0.6m/s$, beginning at $360s$ for $40s$. Based on (21) and (24), we choose $J1_{\Sigma_u} = 5.99$ in advance. Consider the CUSUM detector in (23). We need to estimate the airspeed and obtain the error between the estimation and the measurement in fault free state. By calculating the error and the stand deviation, the parameters τ and σ_0 of CUSUM can be determined. Due to space limitations in this paper, we choose the $J2_{r_u} = 267$ based on the above statements.

First, we estimate the airspeed $\hat{u}$ using state estimation and obtain the two residuals based on (18) and (22). Fig. 2 shows the filter residual J_{Σ_u} and the CUSUM residual J_{r_u}. According to this figure, before $t = 360s$, the CUSUM signal remains well below the threshold. With the chosen threshold detection, the first signs that indicate the airspeed sensor fault occurred at approximately $t = 360.2s$ according to the blue line. At the same time, the residual J_{Σ_u} always remains well below the chosen threshold. It is obvious that there is a fault in the pitot tube at $t = 360s$. From these results, we can conclude that these two residuals can provide good performance for the pitot tube fault diagnosis.

Table 3. Fault detection and isolation logic table

Faulty Sensor	Σ_u	r_u	Σ_α	r_α	Σ_β	r_β	$\Sigma_{\mathbf{a}}$	$r_{\mathbf{a}}$	Σ_ω	r_ω
Pitot tube	√	×								
α-sensor			√	×						
β-sensor					√	×				
Accelerometer							√	×		
Rate Gyro									√	×

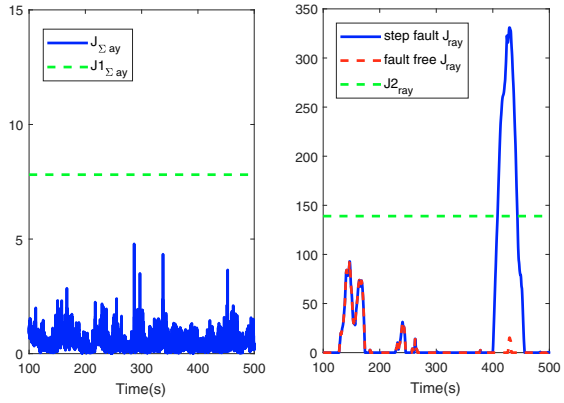

Fig. 3. The accelerometer fault diagnosis

4.2 Fault detection for accelerometer failure

For accelerometer fault diagnosis, we use PMI based input estimation to estimate acceleration a_y. We consider cases where the accelerometer has a bias at $400s$ and the threshold $J1_{\Sigma_{a_y}} = 7.81$ and $J2_{r_{a_y}} = 141$ is chosen. Fig. 3 shows that the residual $J_{\Sigma_{a_y}}$ and the CUSUM residual $J_{r_{a_y}}$. Note that the CUSUM residual $J_{r_{a_y}}$ jumps exceeding the threshold at $t = 400s$ when the bias begins and the residual $J_{\Sigma_{a_y}}$ always remains below the chosen threshold. The acceleromter fault can be easily detected.

5. CONCLUSIONS

In this paper, we presented a method for detecting UAV sensor faults using state and input estimation. We used the EKF and PMI based input estimation to estimate states and inputs, respectively. For the estimation framework, we used the kinematics to formulate a nonlinear state space system. The fault detection logic is constructed for faulty pitot tube, wind vanes and IMU. In order to illustrate sensor fault detection, we used Ultra Stick 25e UAV and presented cases for detecting stuck and bias sensor faults. For the pitot tube and accelerometers, we showed that the sensor residual can be used to detect sensor faults. For other sensors, this proposed approach can also give good performance.

REFERENCES

Basseville, M., and Nikiforov, I. (1993). *Detection of Abrupt Changes: Theory and Application*. NJ, USA: Prentice Hall.

Brumback, B., and Srinath, M. (1987). A fault tolerant multisensor navigation system design. *IEEE Transactions on Aerospace and Electronic Systems*, 23(6), 738-755.

Campa, G., Fravolini, M.L., Seanor, B., et al. (2002). Online learig neural networks for sensor validation for the flight control system of a B777 research scale model. *International Journal of Robust and Nonlinear Control*, 12(11), 987-1007.

Cao, D., Fu, J., and Li, Y. (2017). Fault diagnosis of actuator of Flight Control System based on analytic model. IEEE Proc. Guidance, Navigation and Control Conference, Nanjing, China, pages 397-400.

Castaldi, P., Mimmo, N., Naldi, R., and Marconi, L. (2016). NLGA-based detection and isolation of actuator and sensor faults for quadrotors. IEEE Proc. Decision and Control, Osaka, Japan, pages 3822-3827.

Chen, F., Jiang, R., Zhang, K., Jiang, B., and Tao, G. (2016). Robust backstepping sliding-mode control and observer-based fault estimation for a quadrotor UAV. *IEEE Transactions on Industrial Electronics*, 63(8), 5044-5056.

Chen, Y., Zhang, C., Zhang, Q., and Hu, X. (2017). UAV fault detection based on GA-BP neural network. IEEE Proc. Youth Academic Annual, Hefei, China, pages 806-811.

Deckert, J., Desai, M., Deyst, J., and Willsky, A. (1977). F-8 DFBW sensor failure identification using analytic redundancy. *IEEE Transactions on Automatic Control*, 22(5), 795-803.

Fan, H., Fang, H., Dong, Y. and Ren, S. (2017). UAV engine fault and diagnosis with parmeter models based on telemetry data. IEEE Proc. Prognostics and System Health Management, Harbin, China, pages 1-6.

Gao, Z., and Ding, S.X. (2007). Fault estimation and fault tolerant control for discriptor systems via proportional, multiple-integral and derivative observer design. *IET Control Theory Applicaion*, 1(5), 1208-1218.

Hajiyev, C., and Caliskan, F. (2003). *Fault Diagnosis and Reconfiguration in Flight Control Systems*. Boston, USA: Springer.

Magill, D.T. (1965). Optimal adaptive estimation of sampled stochastic processes. *IEEE Transactions on Automatic Control*, 10(4), 434-439.

Maybeck, P.S. (1999). Multiple model adaptive algorithms for detecting and compensating sensor and actuator failures in aircraft flight control systems. *International Journal of Robust Nonlinear Control*, 9(14), 1051-1070.

Rossi, M., and Brunelli, D. (2016). Autonomous gas detection and mapping with unmanned aerial vehicles. *IEEE Transactions on Instrumentation and measurement*, 65(4), 765-775.

Stevens, B., Lewis, F., and Johnson, E. (2016). *Aircraft Control and Simulation, Dynamics, Controls Design, and Autonomous Systems*. Hoboken, NJ: John Wiley Sons.